frontiers in Astronomy and Space Sciences

ORIGINAL RESEARCH
published: 13 September 2019
doi: 10.3389/fspas.2019.00060

Energy Conversion at Kinetic Scales in the Turbulent Magnetosheath

Zoltán Vörös[1,2]*, *Emiliya Yordanova*[3], *Yuri V. Khotyaintsev*[3], *Ali Varsani*[1] and *Yasuhito Narita*[1]

[1] Space Research Institute, Austrian Academy of Sciences, Graz, Austria, [2] Geodetic and Geophysical Institute, Hungarian Academy of Sciences, Sopron, Hungary, [3] Swedish Institute of Space Physics, Uppsala, Sweden

The process of conversion or dissipation of energy in nearly collisionless turbulent space plasma, is yet to be fully understood. The existing models offer different energy dissipation mechanisms which are based on wave particle interactions or non-resonant stochastic heating. There are other mechanisms of irreversible processes in space. For example, turbulence generated coherent structures, e.g., current sheets are ubiquitous in the solar wind and quasi-parallel magnetosheath. Reconnecting current sheets in plasma turbulence are converting magnetic energy to kinetic and thermal energy. It is important to understand how the multiple (reconnecting) current sheets contribute to spatial distribution of turbulent dissipation. However, detailed studies of such complex structures have been possible mainly via event studies in proper coordinate systems, in which the local inflow/outflow, electric and magnetic field directions, and gradients could be studied. Here we statistically investigate different energy exchange/dissipation (EED) measures defined in local magnetic field-aligned coordinates, as well as frame-independent scalars. The presented statistical comparisons based on the unique high-resolution MMS data contribute to better understanding of the plasma heating problem in turbulent space plasmas.

Keywords: plasma turbulence, current sheets, magnetic reconnection, terrestrial magnetosheath, plasma heating

OPEN ACCESS

Edited by:
Antonella Greco, Department of Physics, University of Calabria, Italy

Reviewed by:
Yan Yang, Southern University of Science and Technology, China
Anton Artemyev, Space Research Institute (RAS), Russia

***Correspondence:**
Zoltán Vörös
zoltan.voeroes@oeaw.ac.at

Specialty section:
This article was submitted to Space Physics, a section of the journal Frontiers in Astronomy and Space Sciences

Received: *30 June 2019*
Accepted: *30 August 2019*
Published: *13 September 2019*

Citation:
Vörös Z, Yordanova E, Khotyaintsev YV, Varsani A and Narita Y (2019) Energy Conversion at Kinetic Scales in the Turbulent Magnetosheath. Front. Astron. Space Sci. 6:60. doi: 10.3389/fspas.2019.00060

1. INTRODUCTION

Turbulence represents an unsolved problem in classical physics of continuous media (e.g., fluids) characterized by velocity shears, intermittent distribution of kinetic energy over multiple spatial, and temporal scales involving strong non-linear interactions and many (possibly infinite) degrees of freedom (e.g., Frisch, 1995). Natural fluid or gaseous flows have both laminar and turbulent components. Some examples are the atmospheric/oceanic circulation, the blood flow, turbulent river flows, turbulent flows in engineering, industrial and laboratory settings, etc. In natural and artificial flows the turbulence strength usually plays a decisive role determining the overall dynamical behavior of a given system. Turbulence in astrophysical systems is also expected to affect the dynamical behavior of plasmas over multiple scales, for example, modifying transport processes or supporting large-scale instabilities (Brandenburg and Lazarian, 2013). On the Sun, among others, turbulence can play a role in coronal heating, solar wind expansion (Cranmer et al., 2015) and particle acceleration (Vlahos et al., 2019). *In-situ* observations of solar wind fluctuations near the ecliptic and at high latitudes revealed scaling and intermittency features resembling the large-scale properties of hydrodynamic turbulence (Tu and Marsch, 1995; Bruno and Carbone, 2013). Within the terrestrial magnetosphere, because of the limited volumes and boundaries, the large fluid-scale scaling features of turbulent fluctuations might be less accessible

(Vörös et al., 2007). Nevertheless, plasma turbulence in the geospace environment also plays a significant role in plasma transport and energization (Borovsky and Funsten, 2003; Vörös et al., 2006; Zimbardo et al., 2010). Space plasma turbulence significantly differs from neutral fluid turbulence in several aspects. It contains a magnetic field which introduces anisotropies into turbulent fluctuations and it is nearly collisionless. In the absence of collisions the dissipation of energy and heating of plasma is rather different from the collisional dissipation in neutral fluids (Howes et al., 2008; Alexandrova et al., 2013; Parashar et al., 2015). The basically collisionless energy transfer processes at kinetic scales happen through wave-field-fluctuation particle interactions, including Landau damping (Chen et al., 2009; Schekochihin et al., 2009), cyclotron damping (Hollweg and Markovskii, 2002) and stochastic heating (Chandran et al., 2010; Hoppock et al., 2018; Schekochihin et al., 2018). Particle energization and heating can happen at (reconnecting) current sheets (Dmitruk et al., 2004; Retino et al., 2007; Servidio et al., 2009; Osman et al., 2012) generated by turbulence through self-organization (Matthaeus et al., 2015). Current sheets observed in the turbulent solar wind (Greco et al., 2009; Servidio et al., 2011) and in the turbulent magnetosheath downstream of a quasi-parallel shock (Chasapis et al., 2015; Vörös et al., 2016; Stawarz et al., 2019) are ubiquitous.

In this paper, using high-resolution field and plasma data from the Magnetospheric Multi-Scale (MMS) mission we investigate derived energy exchange/dissipation measures at (reconnecting) current sheets in the turbulent quasi-parallel magnetosheath. The paper is organized as follows. Section 2 explains the data and instrumentation and section 3 introduces the EED measures and their time evolution during a more than 4 min long time interval in the turbulent magnetosheath. Section 4 presents a conditional statistics of averaged EED measures for normalized current densities. Section 5 contains the summary and conclusions.

2. DATA AND INSTRUMENTATION

We consider the time interval between 00:21:45 and 00:26:15 UT on November 30, 2015, when the MMS spacecraft were in the strongly compressed quasi-parallel magnetosheath. The MMS fleet was at the GSE position (9, –3, –0.5) R_E in tetrahedron configuration with inner probe separation between 4 and 22 km comparable to the electron and ion inertial lengths of ∼1 and 20 km, respectively. During the selected time interval the ion and electron moments with time resolution of 150 and 30 ms, respectively, are available from Fast Plasma Investigation (FPI) instrument (Pollock et al., 2016). The electric field data from Electric Double Probes (EDP) instrument are available with time resolution of 8 kHz (Ergun et al., 2016; Lindqvist et al., 2016; Torbert et al., 2016b). The merged digital fluxgate (FGM) (Russell et al., 2016) and search coil (SCM) (Contel et al., 2016) data were developed by using instrument frequency and timing models that were created during the FIELDS integration test campaign (Fischer et al., 2016; Torbert et al., 2016b). The merged magnetic data analyzed here consists of FGM measurements below 4 Hz and data from SCM between 1 Hz and 6 kHz.

Figure 1 contains the field and plasma data for the selected period of time. **Figures 1A,E** show the GSE components of the magnetic field and of the electric field from MMS1 spacecraft. **Figures 1B–D** are quantities calculated from multi-point spacecraft measurement. **Figure 1B** contains the magnetic shear angles θ_{ij} obtained between spacecraft pairs MMS2-1, 3-1, and 4-1. **Figures 1C,D** show the magnitude of the magnetic field curvature (curvB) and curlometer current density (**J**curl) GSE components, calculated by using the well-known four-point techniques (Dunlop et al., 1988; Chanteur, 1998). The rest of the subplots show electron (**Figures 1F–H**) and ion (**Figures 1I–K**) omnidirectional differential energy flux spectrograms, temperature (including parallel and perpendicular values to the magnetic field) and velocity data, respectively. All parameters show high variability, including the electron and ion energy flux spectrograms. The electron velocity (**Figure 1H**) fluctuates more than the ion velocity (**Figure 1K**), which indicates the presence of electron scale structures in the magnetosheath. The temperature anisotropy is stronger for the electrons (**Figure 1G**) than for the ions (**Figure 1J**), showing preferential electron heating in the parallel direction.

On the X axis of **Figure 1G** four time intervals are highlighted: (a) Quiet interval (after 00:22:18 UT indicated by brown color) when θ_{ij}, curvB, **E**, and **J**curl are small, which means that the spacecraft do not cross any current sheets; (b) Time interval 1 (red color), the enhanced currents, magnetic shear and curvature are associated with reconnecting current sheet exhibiting a full set of fluid and kinetic scale signatures of magnetic reconnection (Vörös et al., 2017); (c) Time interval 2 (red color) contains a strong current sheet associated with electron acceleration parallel to the magnetic field, without clear signatures of ongoing reconnection (Eriksson et al., 2016); (d) Time interval 3 (red color), here ion and electron scale signatures of magnetic reconnection (Yordanova et al., 2016). During the studied active time intervals 1–3 localized enhancements of electron and proton temperatures were also observed. From the ion energy flux spectrogram (**Figure 1I**), it is also visible that occasionally the most energetic ions appear first, such dispersed ion can be generated by remote sources (Vörös et al., 2017). Such dispersion features in the electron energy flux spectrogram are not seen (**Figure 1F**). Relative to the currents in the quiet time interval there are multiple enhancements of the current density frequently associated with rotation of the magnetic field and enhanced curvB (**Figures 1B–D**). Therefore, it is meaningful to further investigate how these current structures are associated with energy conversion/dissipation processes.

3. EED (ENERGY EXCHANGE/DISSIPATION) MEASURES

The electron momentum equation in a two-fluid collisionless plasma can be expressed in the form (Gurnett and Bhattacharjee, 2005):

$$\mathbf{E} + \mathbf{V}_e \times \mathbf{B} = -\frac{1}{qN}\nabla.\mathbb{P}_e + \frac{m_e}{qN}\left(\frac{\partial \mathbf{J}}{q\partial t} + \nabla.N(\mathbf{V}_i\mathbf{V}_i - \mathbf{V}_e\mathbf{V}_e)\right) \quad (1)$$

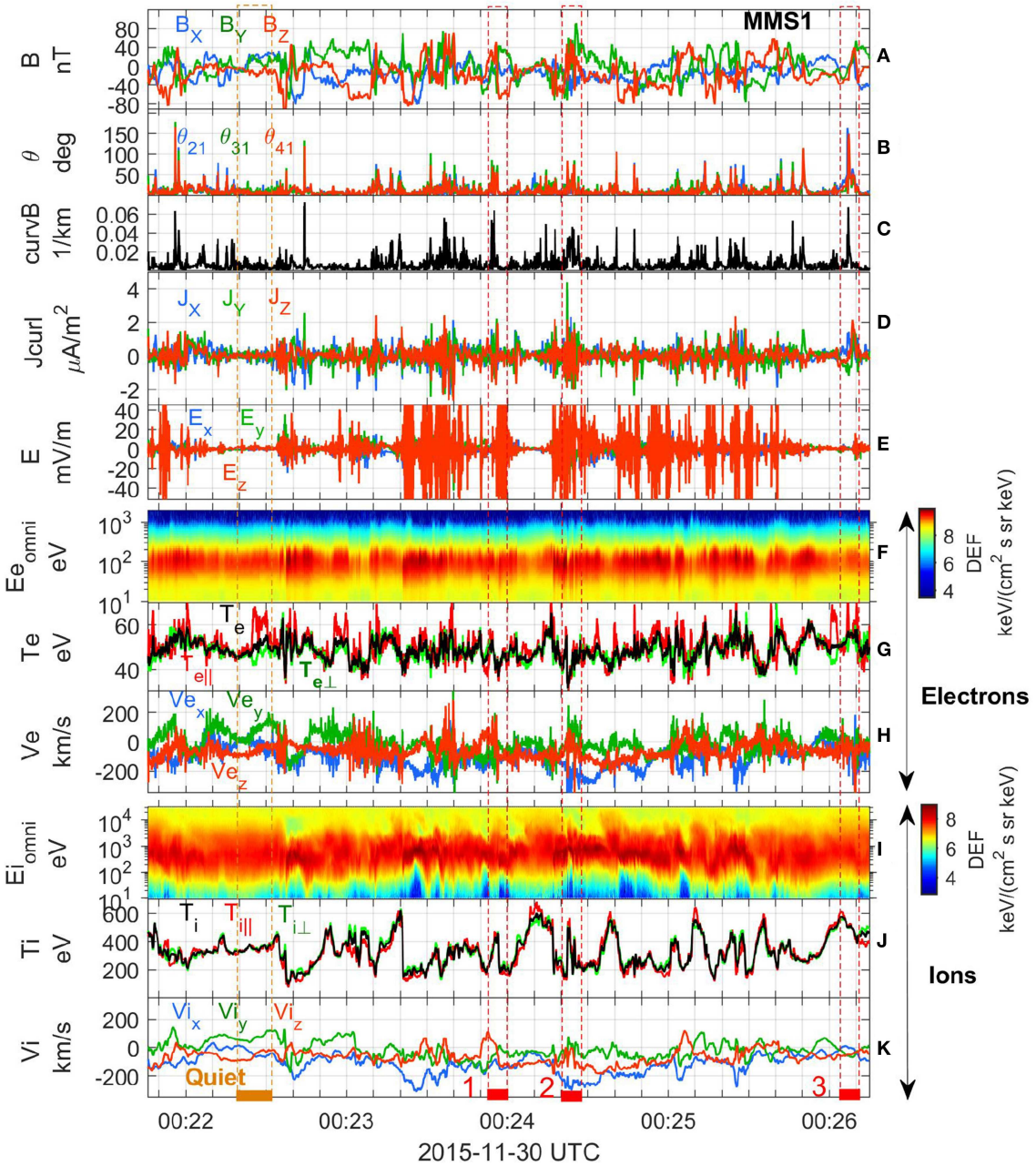

FIGURE 1 | Overview of the event. **(A)** magnetic field components in GSE (B_X, B_Y, B_Z); **(B)** magnetic shear angle between spacecraft pairs θ; **(C)** magnetic field curvature curvB; **(D)** curlometer current density components in GSE (J_X, J_Y, J_Z) **(E)** electric field components in GSE (E_X, E_Y, E_Z); **(F)** omnidirectional electron differential energy flux spectrogram; **(G)** electron temperature (T_e), parallel ($T_{e||}$) and perpendicular ($T_{e\perp}$) to magnetic field electron temperatures; **(H)** electron velocity components in GSE (Ve_X, Ve_Y, Ve_Z); **(I)** omnidirectional ion differential energy flux spectrogram; **(J)** ion temperature (T_i), parallel ($T_{i||}$) and perpendicular ($T_{i\perp}$) to magnetic field ion temperatures; **(K)** ion velocity components in GSE (Vi_X, Vi_Y, Vi_Z).

where $\mathbf{E}' = \mathbf{E} + \mathbf{V}_e \times \mathbf{B}$ is the electric field in the moving frame of electrons, $\mathbb{P}_e$ is the electron pressure tensor, N is the plasma density and the last term which is proportional to the mass of electrons (m_e), the electron inertia term, is negligible when the spatial scale lengths are greater than the electron inertial length. Since collisionless reconnection is associated with multi-scale physics, the ion and electron scales are important in describing the electric fields and currents. In this paper we neglect the last term in Equation (1) and we consider the two remaining terms for constructing the EED measures:

$$\mathbf{J}.\mathbf{E}' \tag{2}$$

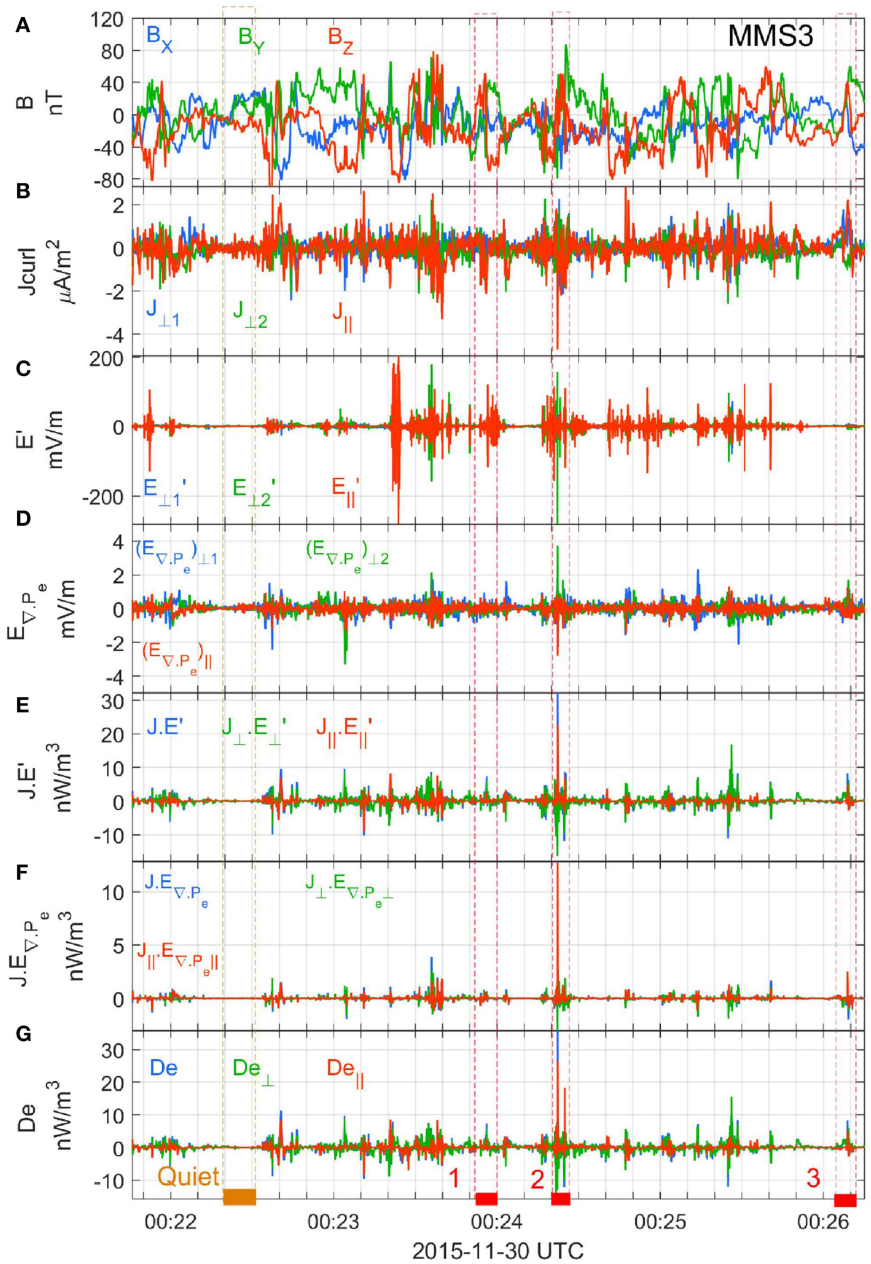

FIGURE 2 | (A) magnetic field components in GSE (B_X, B_Y, B_Z); **(B)** curlometer current density components in field-aligned (FAC) coordinates ($J_{\perp 1}$, $J_{\perp 2}$, $J_{||}$); **(C)** electric field in the moving electron frame $\mathbf{E}' = \mathbf{E} + \mathbf{V_e} \times \mathbf{B}$ in FAC coordinates; **(D)** electric field calculated from the divergence of electron pressure tensor ($E_{\nabla.P_e}$) in FAC coordinates; **(E–G)** EED measures; **(E)** $\mathbf{J}.\mathbf{E}'$ and the perpendicular and parallel products (Equation 2); **(F)** $\mathbf{J}.(-\frac{1}{qN}\nabla.\mathbb{P}_e)$ and the perpendicular and parallel products (Equation 3); **(G)** D_e (Equation 4).

and

$$J.E_{\nabla.P_e} \equiv \mathbf{J}.\left(-\frac{1}{qN}\nabla.\mathbb{P}_e\right) \tag{3}$$

which correspond to the rate of work done by non-ideal part of electric field on plasma particles. Here $\nabla.\mathbb{P}_e$ was again calculated by using the four-point techniques (Chanteur, 1998). Both quantities are used in studies of energy conversion rates associated with magnetic reconnection (e.g., Burch et al., 2016; Torbert et al., 2016a). However, the energy exchange processes in turbulent collisionless plasmas can be more complicated. Recent particle in cell simulations indicate that the pressure-stress interactions can also channel the energy of turbulent fluid motions to plasma particles and this type of energy transfer is preferentially localized at coherent structures (Yang et al., 2017). A recent study by Chasapis et al. (2018) has suggested that perhaps both channels of energy conversion, the work by electromagnetic fields and the effects of pressure-stress

interactions can be analyzed by using the high resolution MMS data. The pressure-stress interactions describe the transfer of energy from multi-scale fluid motions (possibly via a turbulent cascade) to thermal energy and depend on the pressure tensor and velocity gradients. While this energy conversion channel can also be important in collisionless space plasmas (Chasapis et al., 2018), we believe more studies would be needed to optimize the multi-spacecraft separations to properly estimate the underlying scales and velocity gradients. In this paper the pressure-stress terms are not considered. On the other hand, we also consider the frame independent measure introduced by Zenitani et al. (2011):

$$D_e = \mathbf{J}.\mathbf{E}' - q(Ni - Ne)(\mathbf{V}_e.\mathbf{E}') \quad (4)$$

which is similar to Equation (2), however, Equation (4) contains the additional second term on the right side corresponding to the work associated with the transport of net charge. For the time interval considered here the mean value of this term is $\sim$ 0 nW/m^3 with dispersion of $\sim$ 0.7 nW/m^3 (not shown). We note that the average values of electron and ion densities are rather high and approximately equal to $\sim$ 100 1/cm^3, therefore the plasma moments are well determined.

Figures 2A,B contain the magnetic field and curlometer current density components. In **Figures 2C–G** the non-ideal electric field components and the EED measures (Equations 2–4) are shown. Since the goal is to perform a statistical analysis, the field-aligned coordinate system (FAC) is chosen in which the currents, electric fields and the derived measures are transformed to parallel and two perpendicular components relative to the local mean magnetic field. Before calculating the EED measures the electric fields were filtered using a fourth-order elliptic low-pass filter. This removes the high-frequency part of the electric field fluctuations over 1 Hz which can be associated with electrostatic noise or waves. In this way, also the unpredictable effect of stochastic high-frequency fluctuations of the electric field on the dot products in Equations (2–4) is reduced. Since the field aligned and field perpendicular EED measures can be associated with different physical processes (Ergun et al., 2018), in calculating the dot products the parallel and perpendicular components of currents and electric fields are taken, for example, $J_{||}.E'_{||}$ and $J_{\perp}.E'_{\perp}$. To make the calculations possible for the whole time interval the perpendicular directions 1 and 2 are not distinguished.

Figure 2 demonstrates that during the quiet time interval (after 00:22:18 UT, indicated in **Figure 2G**), in the absence of current structures, the EED measures (**Figures 2E–G**) remain close to zero. The previously reported (reconnecting) current sheet events, time intervals 1,2,3, are all associated with elevated values of EED measures. The largest deviations of the measures are associated with the strongest currents during the event 2.

Figures 3A–C show the histograms of the EED measures, separately for the dot products (blue color), the perpendicular (green color) and the parallel (red color) products, respectively. Data for MMS3 spacecraft are shown. The broader distribution corresponds to $\mathbf{J}.\mathbf{E}'$ as it is larger over the sub-ion scales than

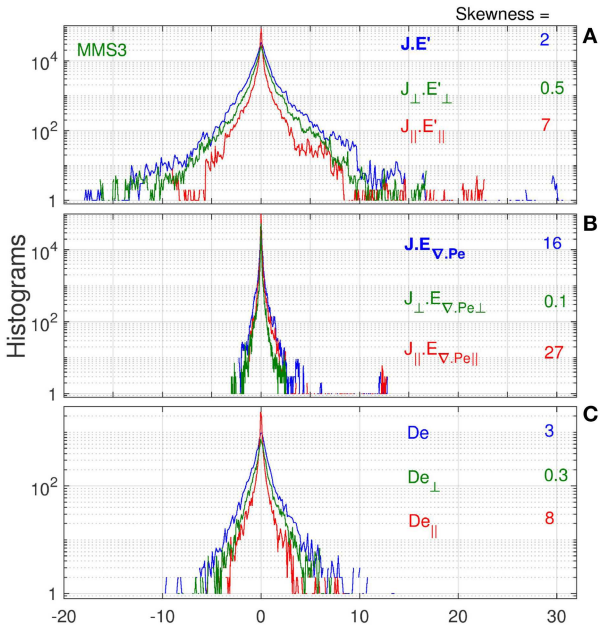

FIGURE 3 | (A–C) Histograms of EED measures and their perpendicular and parallel products from MMS3 sapcecraft; The color coded skewness associated with a histogram is shown for each component on the right.

$\mathbf{J}.\left(-\frac{1}{qN}\nabla.\mathbb{P}_e\right)$ and also it does include some contributions from the fluid scale stresses. For each subplot and product type the skewness of the distributions are shown on the right. The positive skewness means that the distributions have longer tails in positive direction with the meaning that there might exist a net dissipation in the overall energy exchange processes in the turbulent magnetosheath. The largest skewness are associated with EED measures in parallel to magnetic field direction.

4. CONDITIONAL STATISTICS

The goal of the paper is to determine how the local dissipation depends on the strength of the current density in turbulence. To this end we calculated the time averaged EED measures conditioned on current density and normalized to the time averages of the same measure over the whole time interval. In other words, the relative local enhancements of EED measures for certain values of current densities are estimated relative to the background fluctuations of EED measures, for examples $< \mathbf{J}.\mathbf{E}'|J > / < \mathbf{J}.\mathbf{E}' >$. These quantities are plotted against the normalized current density $|\mathbf{J}|/|\mathbf{J}|_{rms} \equiv J/J_{rms}$, where J_{rms} is the root mean square. For each EED measure and MMS1-4 spacecraft the parallel (triangles) and the perpendicular components (circles) of the dot products are shown in **Figures 4A–C**. Again, in dependence on $J/Jrms$ the measures in parallel direction grow faster. The dependence of normalized EED measures averaged in time and over the spacecraft are shown with thick black lines in each subplot. For comparison, in **Figure 4C** the results from 2.5D PIC (magenta color) and

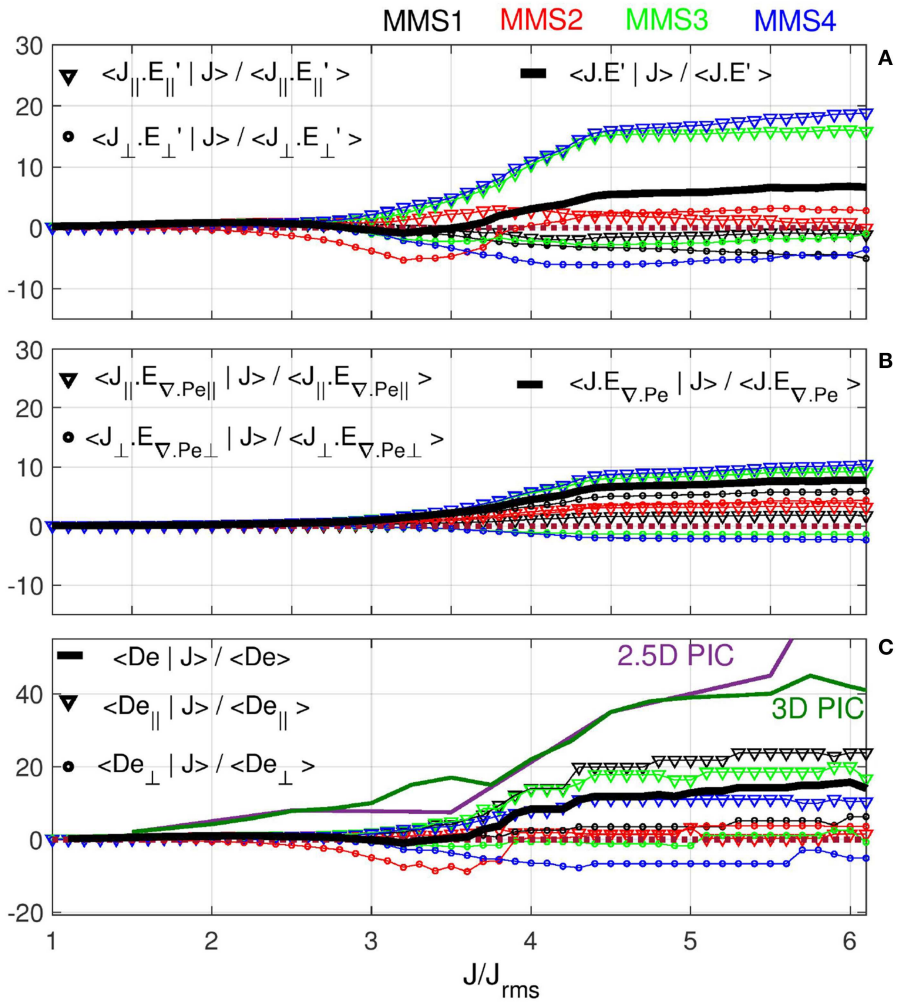

FIGURE 4 | (A–C) Normalized current density J/J_{rms} (rms = root mean square) versus conditional temporal averages of normalized EED measures calculated by conditioning on the values of current density J. The color code in each subplot corresponds to the spacecraft MMS1-4. The triangles show the parallel and the circles the perpendicular products. The thick black lines represent temporal and spatial averages between MMS1-4. In subplot **(C)** the results from 2.5D and 3D PIC simulations are shown (Wan et al., 2015).

3D PIC (green color) are also shown (Wan et al., 2015). It can be seen that in simulations the normalized conditional average $< D_e|J >$ increases faster with J than in the magnetosheath turbulence. However, there is a qualitative agreement, showing that stronger current densities are associated with larger dissipation. This seems to be a valid statement for each EED measure.

In **Figure 4** the EED measures start increasing roughly at $J = 3J_{rms}$ and there are significant differences between components and spacecraft. Actually, $J_{rms} \sim 0.6\ \mu A/m^2$ and for e.g., $4J_{rms}$ the threshold for J is 2.4 $\mu A/m^2$ which corresponds to only a few current sheets in **Figure 2B**. For $J = 6J_{rms} = 3.6\ \mu A/m^2$ it is only one current sheet (event 2 in **Figure 2B**) which enters into the statistics in **Figure 4**, therefore the differences between the spacecraft can be understood as due to different crossing geometries across the same event.

5. SUMMARY AND CONCLUSIONS

In this study more than 4 min of high resolution field and plasma data from the MMS spacecraft was analyzed. Although longer time intervals of magnetosheath data were available from the previous missions, the time resolution of the plasma data was not sufficient to study the thin structures generated by turbulence. The measures corresponding to the work done by electric fields ($\mathbf{J}.\mathbf{E}'$ and $\mathbf{J}.(-\frac{1}{qN}\nabla.\mathbb{P}_e)$) and the corrected measure obtained after removing the net charge transport term (D_e), were estimated. The statistical analysis of the temporally and spatially averaged and normalized measures has shown that there is a net irreversible work done by electric fields at current sheets. The averaged $< D_e|J >$ increases as the current density increases in qualitative agreement with PIC numerical simulations (Wan et al., 2015). However, the time interval under study is rather short

when currents stronger than $5 - 6J_{rms}$ are considered for statistical analysis.

The relative importance of the terms in Equation (1) and of the EED measures in Equations (2–4) have been studied both numerically and experimentally at reconnecting current sheets (Hesse et al., 2016; Nakamura et al., 2016; Shay et al., 2016; Torbert et al., 2016b; Genestreti et al., 2018). According to these event studies, $\mathbf{E}'$ (left hand side of Equation 1) dominates outside the reconnection diffusion region, where both electrons and ions are attached to the magnetic field, and the right hand side of the Equation (1) is negligible. Inside the electron diffusion region, where both ions and electrons are demagnetized, the terms on the right hand side of Equation (1) balance $\mathbf{E}'$ and the first term on the right, $(\nabla.\mathbb{P}_e)$, is much larger than the second inertial term. However, near the reconnection X-line the inertial term can reach half of the pressure divergence term (Genestreti et al., 2018). Since the probability of crossing multiple reconnection X-lines in the magnetosheath is low, the inertial term can be neglected. On the other hand, in terms of EED measures (Equations 2–4), enhanced energy conversion/dissipation can occur not only within the electron diffusion region, but also at reconnection separatrices (Shay et al., 2016). Obviously, when the focus is on understanding of the statistics of dissipation occurring at multiple current sheets in the turbulent magnetosheath the geometry of crossings or the proper coordinate systems of local current sheets cannot be controlled. Our results show that in the quasi-parallel magnetosheath the electric fields (left and right hand sides of Equation 1) and the EED measures are intermittently enhanced. At the same time $\mathbf{E}' \gg E_{\nabla.P_e}$ (**Figures 2C,D**) and except for the current sheet during time interval 2, $\mathbf{J}.\mathbf{E}' > D_e > J.E_{\nabla.P_e}$ (**Figures 2E–G**, **3**). The comparison of histograms in **Figures 3A,C** shows that the distribution of D_e is narrower than the distribution of $\mathbf{J}.\mathbf{E}'$, moreover, the tails of the histograms are also different. However, the comparison of the averaged and normalized EED measures at current sheets in **Figure 4** shows that, for stronger currents, D_e is slightly larger than $\mathbf{J}.\mathbf{E}'$. The EED measures with net positive kurtosis (**Figure 3**) and irreversible work at current sheets (**Figure 4**) indicate that the spacecraft are crossing ion-electron scale current structures, reconnecting current sheets or reconnection separatrices in the turbulent magnetosheath. In fact, case studies have already shown that during the time interval 2 the MMS spacecraft touched the outer electron diffusion region (Vörös et al., 2017) and during the time interval 3 MMS went through a reconnection separatrix (Yordanova et al., 2016).

It was also found that during the analyzed time interval dissipation occurred preferentially in parallel direction to the magnetic field. This is seen in **Figure 1G**, where $T_{e||} > T_{e\perp}$, but mainly in **Figures 3**, **4**, where the statistics of EED measures is presented. In a similar study by Ergun et al. (2018) it was found that the net dissipation in the Earth's plasma sheet was mainly associated with the perpendicular contribution of $\mathbf{J}.\mathbf{E}'$ and the parallel part represented merely 20% of dissipation. However, Ergun et al. (2018) did not apply any conditioning on current sheets for their EED measure. Also, on the basis of Cluster observations of magnetic reconnection in the Earth's magnetotail (Fu et al., 2017) found that in terms of $\mathbf{J}.\mathbf{E}' > 0$ energy dissipation occurred at current filaments, at spiral nulls (O-lines) mainly in perpendicular direction to the magnetic field. However, near radial nulls (X-lines) energy dissipation was surprisingly small. Although in our case the dissipation occurred mainly in the parallel to magnetic field direction, at some MMS spacecraft the EED measures also show net positive dissipation in perpendicular direction as well. Again, in a statistical analysis which includes multiple current sheets the crossings of particular locations of the underlying structures cannot be controlled. Also, the magnetic shear angles ($< 180^\circ$) in **Figure 1B** indicate, that at least over the MMS separation distances, the magnetic field associated with the current sheets is not fully antiparallel and significant guide fields can exist. A reconnection event study has shown that the guide field during time interval 1 reached ∼20% of the main magnetic field (Vörös et al., 2017). Recently, in a statistical study of magnetic reconnection events in the turbulent magnetosheath, Phan et al. (2018) have shown that out of 34 events 23 were associated with magnetic shear angles $<45^\circ$. We can speculate that in turbulent space plasmas the chaotic motions typically generate current sheets with significant guide fields. Both numerical simulations (Shay et al., 2014) and data analysis (Phan et al., 2013; Wilder et al., 2018) show that a guide field suppresses electron perpendicular heating and supports parallel heating. This could explain our observations of preferred parallel heating and energy conversion at magnetosheath current sheets.

Although our understanding of the energy conversion mechanisms at current sheets has improved over the past years, we are far from seeing the complete picture of the associated turbulent dissipation. We mention here two limiting factors. First, the generating mechanisms of current sheets and the role of velocity gradients needs to be understood better. Second, reconnecting current sheets in 3D turbulence can be associated with electron scale coherent structures, for example, interacting extended flux ropes (Daughton et al., 2011). In both cases the one-scale tetrahedron geometry (Cluster or MMS) appears to be a limiting factor in the observation of real multi-scale 3D processes.

Certainly, further numerical simulations, event studies and statistical analysis of current sheets will be needed to understand better the role of coherent structures in kinetic energy conversions in collisionless turbulent plasmas and their contribution to the total heating of larger plasma volumes.

DATA AVAILABILITY

The datasets analyzed for this study can be found in the MMS science data archive https://lasp.colorado.edu/mms/sdc/public/.

AUTHOR CONTRIBUTIONS

ZV and EY analyzed the data and drafted the manuscript. YK, AV, and YN contributed to the interpretation of the analysis and general improvements in the manuscript.

FUNDING

ZV was supported by the Austrian FWF project P28764-N27. EY was supported by the Swedish Civil Contingencies Agency, grant 2016-2102.

ACKNOWLEDGMENTS

We are grateful for numerous discussions on this topic with R. Nakamura and O. W. Roberts, both from Space Research Institute, Graz.

REFERENCES

Alexandrova, O., Chen, C., Sorriso-Valvo, L., Horbury, T., and Bale, S. (2013). Solar wind turbulence and the role of ion instabilities. *Space Sci. Rev.* 178, 101–139. doi: 10.1007/s11214-013-0004-8

Borovsky, J., and Funsten, H. (2003). Mhd turbulence in the earths plasma sheet: dynamics, dissipation and driving. *J. Geophys. Res.* 108, 1–37. doi: 10.1029/2002JA009625

Brandenburg, A., and Lazarian, A. (2013). Astrophysical hydromagnetic turbulence. *Space Sci. Rev.* 178, 163–200. doi: 10.1007/s11214-013-0009-3

Bruno, R., and Carbone, V. (2013). The solar wind as a turbulence laboratory. *Living Rev. Sol. Phys.* 10, 1–208. doi: 10.12942/lrsp-2013-2

Burch, J. L., Torbert, R. B., Phan, T. D., Chen, L. L., Moore, T. E., Ergun, R. E., et al. (2016). Electron-scale measurements of magnetic reconnection in space. *Science* 352, aaf2939–1–aaf2939–10. doi: 10.1126/science.aaf2939

Chandran, B., Li, B., Rogers, B., Quataert, E., and Germaschewski, K. (2010). Perpendicular ion heating by low-frequency alfven wave turbulence in the solar wind. *Astrophys. J.* 720, 503–515. doi: 10.1088/0004-637X/720/1/503

Chanteur, G. (1998). "Spatial interpolation for four spacecraft: theory," in *Analysis Methods for Multi-Spacecraft Data,* eds G. Paschmann and P. Daly (Bern; Noordwijk: ISSI/ESA Publications Division), 349–369.

Chasapis, A., Retino, A., Sahraoui, F., Vaivads, A., Khotyaintsev, Y., Sundkvist, D., et al. (2015). The current sheets and associated electron heating in turbulent space plasma. *Astrophys. J. Lett.* 804, 1–5. doi: 10.1088/2041-8205/804/1/L1

Chasapis, A., Yang, Y., Matthaeus, W., Parashar, T., Haggerty, C., Burch, J., et al. (2018). Energy conversion and collisionless plasma dissipation channels in the turbulent magnetosheath observed by the magnetospheric multiscale mission. *Astrophys. J.* 862, 1–7. doi: 10.3847/1538-4357/aac775

Chen, C. H. K., Klein, K. G., and Howes, G. G. (2009). Evidence for electron landau damping in space plasma turbulence. *Nat. Com.* 10, 1–8. doi: 10.1038/s41467-019-08435-3

Contel, O. L., Leroy, P., Roux, A., Coillot, C., Alison, D., Bouabdellah, A., et al. (2016). The search-coil magnetometer for MMS. *Space Sci. Rev.* 199, 257–282. doi: 10.1007/978-94-024-0861-4-9

Cranmer, S. R., Asgari-Targhi, M., Miralles, M. P., Raymond, J. C., Strachan, L., Tian, H., et al. (2015). The role of turbulence in coronal heating and solar wind expansion. *Phil. Trans. R. Soc. A* 373, 1–16. doi: 10.1098/rsta.2014.0148

Daughton, W., Roytershteyn, V., Karimabadi, H., Yin, L., Albright, B., Bergen, B., et al. (2011). Role of electron physics in the development of turbulent magnetic reconnection in collisionless plasmas. *Nat. Phys.* 7, 539–542. doi: 10.1038/nphys1965

Dmitruk, P., Matthaeus, W., and Seenu, N. (2004). Test particle energization by current sheets and nonuniform fields in magnetohydrodynamic turbulence. *Astrophys. J.* 617, 667–679. doi: 10.1086/425301

Dunlop, M., Southwood, D., Glassmeier, K., and Neubauer, F. (1988). Analysis of multipoint magnetometer data. *Adv. Space Res.* 8, 273–277. doi: 10.1016/0273-1177(88)90141-X

Ergun, R., Goodrich, K., Wilder, F., Ahmadi, N., Holmes, J., Eriksson, S., et al. (2018). Magnetic reconnection, turbulence, and particle acceleration: observations in the earths magnetotail. *Geophys. Res. Lett.* 45, 3338–3347. doi: 10.1002/2018GL076993

Ergun, R., Tucker, S., Westfall, J., Goodrich, K., Malaspina, D., Summers, D., et al. (2016). The axial double probe and fields signal processing for the MMS mission. *Space Sci. Rev.* 199, 167–188. doi: 10.1007/s11214-014-0115-x

Eriksson, E., Vaivads, A., Graham, D., Khotyaintsev, Y., Yordanova, E., Hietala, H., et al. (2016). Strong current sheet at a magnetosheath jet: kinetic structure and electron acceleration. *J. Geophys. Res. Space Phys.* 121, 9608–9618. doi: 10.1002/2016JA023146

Fischer, D., Magnes, W., Hagen, C., Dors, I., Chutter, M., Needell, J., et al. (2016). Optimized merging of search coil and fluxgate data for MMS. *Geosci. Instrum. Method. Data Syst.* 5, 521–530. doi: 10.5194/gi-5-521-2016

Frisch, U. (1995). *Turbulence: The Legacy of A.N. Kolmogorov*. Cambridge: Cambridge University Press.

Fu, H., Vaivads, A., Khotyaintsev, Y., Andre, M., Cao, J., Olshevsky, V., et al. (2017). Intermittent energy dissipation by turbulent reconnection. *Geophys. Res. Lett.* 44, 37–43. doi: 10.1002/2016GL071787

Genestreti, K., Varsani, A., Burch, J., Cassak, P., Torbert, R., Nakamura, R., et al. (2018). MMS observation of asymmetric reconnection supported by 3-d electron pressure divergence. *J. Geophys. Res.* 123, 1806–1821. doi: 10.1002/2017JA025019

Greco, A., Matthaeus, W., Servidio, S., Chuychai, P., and Dmitruk, P. (2009). Statistical analysis of discontinuities in solar wind ace data and comparison with intermittent mhd turbulence. *Astrophys. J.* 691, L111–L114. doi: 10.1088/0004-637X/691/2/L111

Gurnett, D., and Bhattacharjee, A. (2005). *Introduction to Plasma Physics*. Cambridge: Cambridge University Press.

Hesse, M., Liu, Y., Chen, L., Bessho, N., Kuznetsova, M., Birn, J., et al. (2016). On the electron diffusion region in asymmetric reconnection with a guide magnetic field. *Geophys. Res. Lett.* 43, 2359–2364. doi: 10.1002/2016GL068373

Hollweg, J., and Markovskii, S. A. (2002). Cyclotron resonances of ions with obliquely propagating waves in coronal holes and the fast solar wind. *J. Geophys. Res.* 107, 1–7. doi: 10.1029/2001JA000205

Hoppock, I. W., Chandran, B. D. G., Klein, K. G., Mallet, A., and Verscharen, D. (2018). Stochastic proton heating by kinetic-alfven-wave turbulence in moderately high-beta plasmas. *J. Plasma Phys.* 84, 1–21. doi: 10.1017/S0022377818001277

Howes, G., Cowley, S., Dorland, W., Hammett, G., Quataert, E., and Schekochihin, A. (2008). A model of turbulence in magnetized plasmas: implications for the dissipation range in the solar wind. *J. Geophys. Res.* 113, 1–24. doi: 10.1029/2007JA012665

Lindqvist, P., Olsson, G., Torbert, R., King, B., Granoff, M., Rau, D., et al. (2016). The spin-plane double probe electric field instrument for MMS. *Space Sci. Rev.* 199, 137–165. doi: 10.1007/978-94-024-0861-4-6

Matthaeus, W. H., Wan, M., Servidio, S., Greco, A., Osman, K. T., Oughton, S., et al. (2015). Intermittency, nonlinear dynamics and dissipation in the solar wind and astrophysical plasmas. *Philos. Trans. R. Soc. A* 373, 1–32. doi: 10.1098/rsta.2014.0154

Nakamura, T., Nakamura, R., and Hasegawa, H. (2016). Spatial dimensions of the electron diffusion region in anti-parallel magnetic reconnection. *Ann. Geophys.* 34, 357–367. doi: 10.5194/angeo-34-357-2016

Osman, K. T., Matthaeus, W. H., Wan, M., and Rappazzo, A. F. (2012). Intermittency and local heating in the solar wind. *Phys. Rev. Lett.* 108, 261102–1–261102–4. doi: 10.1103/PhysRevLett.108.261102

Parashar, T., Salem, C., Wicks, R., Karimabadi, H., Gary, S., and Matthaeus, W. (2015). Turbulent dissipation challenge: a community-driven effort. *J. Plasma Phys.* 81, 1–22. doi: 10.1017/S0022377815000860

Phan, T., Shay, M., Gosling, J., Fujimoto, M., Drake, J., Paschmann, G., and et al. (2013). Electron bulk heating in magnetic reconnection at earths magnetopause: dependence on the inflow alfven speed and magnetic shear. *Geophys. Res. Lett.* 40, 4475–4480. doi: 10.1002/grl.50917

Phan, T. D., Eastwood, J. P., Shay, M. A., Drake, J. F., Sonnerup, B., Fujimoto, M., and et al. (2018). Electron magnetic reconnection without ion coupling in earth's turbulent magnetosheath. *Nature* 557, 202–206. doi: 10.1038/s41586-018-0091-5

Pollock, C., Moore, T., Jacques, A., Burch, J., Gliese, U., Saito, Y., et al. (2016). Fast plasma investigation for magnetospheric multiscale. *Space Sci. Rev.* 199, 331–406. doi: 10.1007/s11214-016-0245-4

Retino, A., Sundkvist, D., Vaivads, A., Mozer, F., Andre, M., and Owen, C. (2007). *In situ* evidence of magnetic reconnection in turbulent plasma. *Nat. Phys.* 3, 235–238. doi: 10.1038/nphys574

Russell, C., Anderson, B., Baumjohann, W., Bromund, K., Dearborn, D., Fischer, D., et al. (2016). The magnetospheric multiscale magnetometers. *Space Sci. Rev.* 199, 189–256. doi: 10.1007/s11214-014-0057-3

Schekochihin, A., Cowley, S., Dorland, W., Hammett, G., Howes, G., Quataert, E., et al. (2009). Astrophysical gyrokinetics: kinetic and fluid turbulent cascades in magnetized weakly collisional plasmas. *Astrophys. J. Suppl.* 182, 310–377. doi: 10.1088/0067-0049/182/1/310

Schekochihin, A., Kawazura, Y., and Barnes, M. A. (2018). Constraints on ion versus electron heating by plasma turbulence at low beta. *J. Plasma Phys.* 85, 1–41. doi: 10.1017/S0022377819000345

Servidio, S., Greco, A., Matthaeus, W., Osman, K., and Dmitruk, P. (2011). Statistical association of discontinuities and reconnection in magnetohydrodynamic turbulence. *J. Geophys. Res.* 116, 1–11. doi: 10.1029/2011JA016569

Servidio, S., Matthaeus, W., Shay, M., Cassak, P., and Dmitruk, P. (2009). Magnetic reconnection in two-dimensional magnetohydrodynamic turbulence. *Phys. Rev. Lett.* 102, 115003–1–115003–4. doi: 10.1103/PhysRevLett.102.115003

Shay, M., Haggerty, C., Phan, T., Drake, J., Cassak, P., Wu, P., et al. (2014). Electron heating during magnetic reconnection: a simulation scaling study. *Phys. Plasmas* 21, 122902–1–122902–11. doi: 10.1063/1.4904203

Shay, M., Phan, T., Haggerty, C., Fujimoto, M., Drake, J., Malakit, K., and et al. (2016). Kinetic signatures of the region surrounding the x line in asymmetric (magnetopause) reconnection. *Geophys. Res. Lett.* 43, 4145–4154. doi: 10.1002/2016GL069034

Stawarz, J., Eastwood, J., Phan, T., Gingell, I., Shay, M., Burch, J., et al. (2019). Properties of the turbulence associated with electron-only magnetic reconnection in earths magnetosheath. *Astrophys. J. Lett.* 877, 1–7. doi: 10.3847/2041-8213/ab21c8

Torbert, R., Burch, J., Giles, B., Gershman, D., Pollock, C. J., Dorelli, J., Avanov, L., et al. (2016a). Estimates of terms in ohms law during an encounter with an electron diffusion region. *Geophys. Res. Lett.* 43, 5918–5925. doi: 10.1002/2016GL069553

Torbert, R., Russell, C., Magnes, W., Ergun, R., Lindqvist, P., LeContel, O., et al. (2016b). The fields instrument suite on MMS: scientific objectives, measurements, and data products. *Space Sci. Rev.* 199, 105–135. doi: 10.1007/s11214-014-0109-8

Tu, C., and Marsch, E. (1995). Mhd structures, waves and turbulence in the solar wind: observations and theories. *Space Sci. Rev.* 73, 1–210. doi: 10.1007/978-94-015-8541-5

Vlahos, L., Anastasiadis, A., Papaioannou, A., Kouloumvakos, A., and Isliker, H. (2019). Sources of solar energetic particles. *Philos. Trans. R. Soc. A* 377, 1–26. doi: 10.1098/rsta.2018.0095

Vörös, Z., Baumjohann, W., Nakamura, R., Runov, A., Volwerk, M., Asano, Y., et al. (2007). Spectral scaling in the turbulent earths plasma sheet revisited. *Nonlin. Processes Geophys.* 14, 535–541. doi: 10.5194/npg-14-535-2007

Vörös, Z., Baumjohann, W., Nakamura, R., Volwerk, M., and Runov, A. (2006). Bursty bulk flow driven turbulence in the earths plasma sheet. *Space Sci. Rev.* 122, 301–311. doi: 10.1007/s11214-006-6987-7

Vörös, Z., Yordanova, E., Echim, M., Consolini, G., and Narita, Y. (2016). Turbulence-generated proton-scale structures in the terrestrial magnetosheath. *Astrophys. J. Lett.* 819, 1–6. doi: 10.3847/2041-8205/819/1/L15

Vörös, Z., Yordanova, E., Varsani, A., Genestreti, K., Khotyaintsev, Y., Li, W., et al. (2017). MMS observation of magnetic reconnection in the turbulent magnetosheath. *J. Geophys. Res. Space Phys.* 122, 11442–11467.

Wan, M., Matthaeus, W. H., Roytershteyn, V., Karimabadi, H., Parashar, T., Wu, P., et al. (2015). Intermittent dissipation and heating in 3d kinetic plasma turbulence. *Phys. Rev. Lett.* 114, 1–4. doi: 10.1103/PhysRevLett.114.175002

Wilder, F., Ergun, R., Burch, J., Ahmadi, N., Eriksson, S., Phan, T., et al. (2018). The role of the parallel electric field in electron-scale dissipation at reconnecting currents in the magnetosheath. *J. Geophys. Res.* 123, 6533–6547. doi: 10.1029/2018JA025529

Yang, Y., Matthaeus, W., Parashar, T., Haggerty, C., Roytershteyn, V., Daughton, W., et al. (2017). Energy transfer, pressure tensor, and heating of kinetic plasma. *Phys. Plasmas* 24, 1–14. doi: 10.1063/1.4990421

Yordanova, E., Vörös, Z., Varsani, A., Graham, D., Norgren, C., Khotyainstev, Y., et al. (2016). Electron scale structures and magnetic reconnection signatures in the turbulent magnetosheath. *Geophys. Res. Lett.* 43, 5969–5978. doi: 10.1002/2016GL069191

Zenitani, S., Hesse, M., Klimas, A., Black, C., and Kuznetsova, M. (2011). The inner structure of collisionless magnetic reconnection: the electron-frame dissipation measure and hall fields. *Phys. Plasmas* 18, 1–9. doi: 10.1063/1.3662430

Zimbardo, G., Greco, A., Sorriso-Valvo, L., Perri, S., Vörös, Z., Aburjania, G., et al. (2010). Magnetic turbulence in the geospace environment. *Space Sci. Rev.* 156, 89–134. doi: 10.1007/s11214-010-9692-5

Conflict of Interest Statement: The authors declare that the research was conducted in the absence of any commercial or financial relationships that could be construed as a potential conflict of interest.